Astron. Astrophys. 346, 491–500 (1999)

ASTRONOMY AND ASTROPHYSICS

The chemical composition of the pulsating helium star V652 Her⋆

C. Simon Jeffery[1], **Philip W. Hill**[2], **and Ulrich Heber**[3]

[1] Armagh Observatory, College Hill, Armagh BT61 9DG, Ireland
[2] Department of Physics and Astronomy, St. Andrews University, St Andrews, Fife KY16 9SS, Scotland
[3] Dr. Remeis-Sternwarte, Universität Erlangen-Nürnberg, D-96049 Bamberg, Germany

Received 14 January 1999 / Accepted 31 March 1999

Abstract. We present an analysis of an optical blue spectrum of the pulsating helium star V652 Her (=BD+13°3224) in order to determine its effective temperature, surface gravity and chemical composition. By fitting synthetic spectra to the observations we find that for our spectrum $T_{\rm eff} = 24\,550 \pm 500$ K, $\log g = 3.68 \pm 0.05$ (cgs) and $v_{\rm t} = 5 \pm 5$ km s^{-1}. The surface gravity, together with a previous measurement of the stellar radius, indicates the mass of V652 Her to be $M = 0.69^{+0.15}_{-0.12}\,{\rm M}_{\odot}$. The surface composition is characterised by abundances of $n_{\rm H} = 0.009$, $n_{\rm He} = 0.988$, $n_{\rm C} \simeq 0.000040$, $n_{\rm N} = 0.0025$ and $n_{\rm O} = 0.00010$ (number fractions). These abundances represent a mixture of some hydrogen-rich material (0.2% by mass) with predominantly CNO-processed helium (99.8% by mass). The metallicity of V652 Her, represented by the N abundance as a sum of primordial C+N+O abundances, by the iron abundance, and by other metals, corresponds to a near-solar mixture, with [Fe/H]$= -0.10 \pm 0.15$. Such a metallicity supports the contention that Z-bump opacities drive pulsations in metal-rich helium stars in an instability finger that extends to low luminosities for stars with $T_{\rm eff} \sim 20\,000$ K. There is no evidence for the products of any nuclear processes other than the CNO cycle on the stellar surface. If V652 Her was formed by the merger of two white dwarfs, its surface composition demands that they should both be helium white dwarfs. Conversely, if it is the product of single-star evolution, it is more likely to be a post-giant branch star. In either case it is probably evolving onto the helium main-sequence, with important consequences for understanding the origin of hot subluminous stars. A small discrepancy remains between $T_{\rm eff}$ and $\log g$ measured from the average blue-visual spectrum in this paper, and that measured from UV-optical spectrophotometry previously. Further work will be necessary to resolve this, and to make progress in determining the mass of V652 Her.

Key words: stars: individual: V652 Her – stars: chemically peculiar – stars: abundances

1. Introduction

The phenomenon of pulsation depends critically on the radiative opacity in the outer layers of a star. Discrepancies between theoretical models for evolution and for pulsation of classical Cepheids have driven intensive investigations of atomic processes and calculations of stellar opacity. Since the total radiative opacity is also closely tied to the local chemical composition, opacity calculations which involve many different ion species should ideally be tested over a range of chemical compositions. Nature has dictated that most pulsating variables have a chemical composition fairly similar to that of the Sun, which is dominated by hydrogen. Consequently, pulsations in stars which contain little or no hydrogen provide immensely important tests for pulsation theory and for calculations of the non-hydrogenic component of stellar opacity.

The early-type star V652 Her (=BD+13°3224) was discovered to be hydrogen-deficient by Berger & Greenstein (1963), and to show a 2.5 hour variation by Landolt (1975). Subsequent studies have established that the variations are due to radial pulsation (Hill et al. 1981 = paper I) and have been used to deduce the stellar radius independent of distance (Lynas-Gray et al. 1984 = paper II). Crucially, these studies have indicated that the mass of V652 Her is small ($\sim 0.7\,{\rm M}_{\odot}$) and that it is therefore not related to massive population I Wolf-Rayet stars. The pulsation period has been measured very accurately and been shown to be decreasing (Kilkenny & Lynas-Gray 1982, 1984, Kilkenny 1988, Kilkenny & Marang 1991, Kilkenny et al. 1996) at a rate commensurate with an effective temperature change due to the evolutionary contraction of a low-mass giant (Jeffery 1984). Theoretical linear analyses of the pulsation failed to find any reason for pulsational instability (Saio 1986) until modern opacity calculations included correctly the contribution from iron-group elements around 10^6 K (Rogers & Iglesias 1992). Subsequently, Saio (1993) found that pulsations can be excited in extreme helium stars with effective temperatures ($T_{\rm eff}$) around 20 000 K and luminosities (L) above $\sim 200\,{\rm L}_{\odot}$ (for $M = 0.7\,{\rm M}_{\odot}$, $Z = 0.01$). This result is strongly composition dependent, the low-luminosity limit of this pulsation finger rises with decreasing metallicity (Saio 1995). Thus the helium star HD 144941 is not variable because of its very low metallicity (Jeffery & Hill 1996, Harrison & Jeffery 1997, Jeffery & Har-

Send offprint requests to: C.S. Jeffery

⋆ Based on observations obtained at the Anglo-Australian Telescope, Coonabarabran, NSW, Australia.

Table 1. Summary of spectra used in the analysis of V652 Her, including dates of observation, instrumental setup, wavelength range ($\lambda_{\rm min}-\lambda_{\rm max}$, Å), dispersion ($\delta$, Å/pixel), exposure time (t, seconds), number of spectra (n), signal to noise (1σ) ratio of coadded spectrum (S/N) and total phase coverage ($\Delta\phi$, cycles). The instrument codes are AAT: Anglo-Australian Telescope, RGO: RGO spectrograph, 25: 25cm camera, 82: 82cm camera.

Dates	Instrument+Detector	$\lambda_{\rm min}$	$\lambda_{\rm max}$	δ	t	n	S/N	$\Delta\phi$	Paper
1979 July 12	AAT+RGO82+IPCS	4156	4615	0.25	500	20	90	1.5	I
1980 May 24,25	AAT+RGO82+IPCS	4130	4610	0.25	200	55	70	3.0	II
1982 July 2	AAT+RGO82+IPCS	3892	4163	0.15	300	40	100	2.5	III
1982 July 3	AAT+RGO25+CCD	4180	4570	0.78	200	24	†50	2.5	III
1984 April 15	AAT+RGO82+IPCS	3359	3623	0.15	20	465	70	1.1	III
1984 April 17	AAT+RGO82+IPCS	3579	3849	0.15	20	660	110	1.7	III

† S/N for individual exposures.

rison 1997), whilst the metal-rich helium star LSS 3184 shows pulsations similar to those in V652 Her (Kilkenny & Koen 1995, Drilling et al. 1998). Meanwhile Fadeyev & Lynas-Gray (1996) have made non-linear calculations of the pulsations in V652 Her. They were able to reproduce the detailed velocity curve measured by Jeffery & Hill (1986 = Paper III) remarkably well, with a model $M = 0.72\,{\rm M}_\odot$, $\langle T_{\rm eff}\rangle = 23500\,{\rm K}$ and $\langle L\rangle = 1062\,{\rm L}_\odot$, and with a composition $X = 0.0015, Z = 0.01563$. Angled brackets $\langle\rangle$ represent average values over the pulsation cycle. Whilst it is clear that the pulsations in V652 Her are due to an iron-group opacity bump, detailed pulsation modelling depends heavily upon an accurate knowledge of the surface composition of the star.

Since discovery (Berger & Greenstein 1963) it has been evident that V652 Her is hydrogen poor and nitrogen rich. This in itself is remarkable since practically all other B-type helium stars, with negligible Balmer lines and strong neutral helium lines, show very high carbon abundances. For a star with a hydrogen-poor surface, a nitrogen-rich surface indicates material primarily processed into helium through the CNO cycle, as seen in the WN–type Wolf-Rayet sequence. A carbon-rich surface would indicate a mixture which includes 3α processed material. Being unique amongst extreme helium stars in this respect, V652 Her has therefore been regarded as an exceptional case, and the question arises as to whether its evolution is in any way related to that of other extreme helium stars, itself a major unsolved problem in astronomy. Central to this question is a precise measurement of the surface composition of V652 Her.

Even more crucial to studies of V652 Her is the measurement of mass. This depends upon the radius which was carefully established, independent of distance, in Paper II. It also depends upon an accurate measurement of the stellar surface gravity ($\log g$). Like the surface composition, this depends on a detailed analysis of the optical absorption spectrum. Measurements adopted in Papers I ($\log g = 4.0$) and II ($\log g = 3.7$) have yet to be verified by such an analysis.

Data have been available for a fine analysis of V652 Her since the mid 1980's. Initial attempts to complete this analysis met with partial success (Jeffery et al. 1986, Jeffery 1996), restricted primarily by insufficient physics in the model atmospheres and inappropriate methods for the analysis. Much has been done to improve the model atmospheres and analysis techniques (Jeffery & Heber 1992, Jeffery 1996, Jeffery et al. 1998) to the extent that a robust and self-consistent analysis of the optical spectrum has become possible. This paper reports the results of that analysis.

2. Observations

High-resolution optical spectra were obtained with the Anglo-Australian Telescope using the RGO spectrograph on four observing runs between 1979 and 1984. Full details are given in papers I, II and III and are summarized in Table 1. Here it is sufficient to note that, in all cases, the observations consisted of a series of short exposures in order to measure radial velocities. Individual spectra were velocity corrected to the laboratory rest frame, normalized to the local continuum and then coadded within each observed wavelength region. Data obtained with a CCD on 1982 July 3 were not used in the current analysis because of their low spectral resolution, despite their high S/N ratio.

In order to obtain a spectrum with a signal-to-noise ratio (S/N) sufficiently high for a reliable quantitative analysis, all of the individual spectra within each observing run were coadded. This inevitably led to a biased sampling of the pulsation cycle. There were insufficient individual spectra to obtain sufficient S/N for a satisfactory analysis at specific phases (ϕ), for example in phase bins less than 0.1 cycles duration[1]. Similarly there was insufficient phase coverage to obtain an integrated spectrum with sufficient S/N equally weighted around the pulsation cycle (note the poor coverage around $\phi = 0.3$, Fig. 1).

The coadded spectra were normalized by fitting a low-order spline function to manually identified regions of continuum. For wavelengths greater than ~ 4050 Å the continuum definition is

[1] During early work on this project (Jeffery et al. 1986), two additional spectra were constructed from individual short exposures obtained within ± 0.1 cycles of minimum and maximum $T_{\rm eff}$. Measurements proved to be of limited value, principally because of the absorption lines studied and because of low S/N ratios. However they provided an estimate of the effective temperature variation $\Delta T_{\rm eff} = 2\,400 \pm 500\,{\rm K}$, which should be compared with that obtained from ultraviolet spectrophotometry, averaged over the same phase intervals, in Paper II ($\Delta T_{\rm eff} = 2\,800 \pm 110\,{\rm K}$).

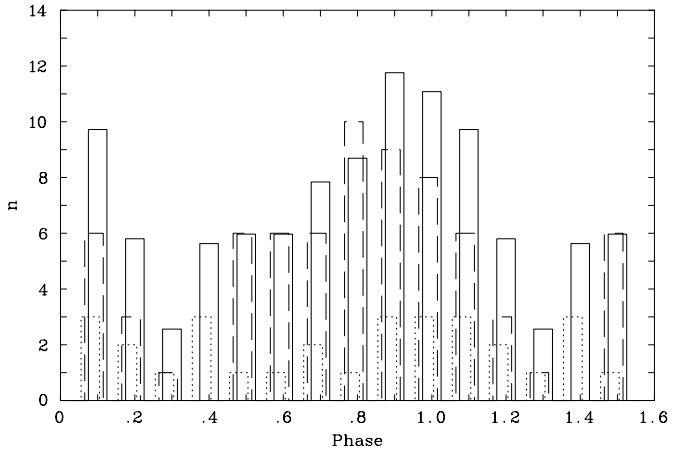

Fig. 1. The distribution with phase of individual IPCS spectra from 1979 (dotted) and 1980 (dashed). The sum weighted by the inverse number of exposures in each observing run (solid line) represents the actual phase coverage of the spectrum analyzed.

satisfactory. The main problem turns out, with hindsight, to be the convolution of line broadening and and a line-rich spectrum, leading to relatively few uncontaminated continuum regions. A subsidiary problem is the possible presence of broad but shallow lines due to ionized helium.

An autocorrelation measurement of the intrinsic line profile in the 1979, 1980 and 1982 IPCS spectra showed good consistency between independent datasets. Line widths of 113, 97 and 74 $\mathrm{km\,s^{-1}}$(FWHM) respectively were obtained, substantially larger than the intrinsic width of theoretical line profiles for a non-rotating static photosphere. Instrumental broadening, measured from the width of lines in the copper-argon comparison lamp, is ~ 1.4 pixels (or $\sim 25\,\mathrm{km\,s^{-1}}$) FWHM. Some additional broadening could be due to incomplete removal of the pulsation velocity shifts, to velocity gradients within the stellar atmosphere. Papers I to III indicate the steps taken to ensure that relative velocity shifts were completely removed – otherwise larger discrepancies between independent datasets could have been expected. Most absorption lines are formed in a narrow layer of the stellar atmosphere, so the mean line profile should not be strongly affected by velocity gradients within the atmosphere.

The various coadded spectra were finally combined to give a single spectrum of moderately high signal-to-noise ratio (~ 100) with almost complete wavelength coverage from 3400 Å to 4600 Å, with a small gap between 3850 and 3890 Å(Fig. 2). Blueward of 4050 Å, the Stark-broadened wings of the neutral helium lines cause severe difficulties, since there is effectively no true continuum between He I λ4026 Å and the limit of the diffuse He I series at ~ 3450 Å. This difficulty is compounded because our spectral modelling software does not yet contain good broadening data for sufficient He I lines. Consequently, these regions of spectrum do not make a major contribution to the present analysis.

Three other sources of line broadening are important. One arises from the convolution of integration time with the acceleration of the atmosphere. In the case of the 500 second exposures obtained in 1979, this amounts to a broadening by a top-hat function with full width $\delta v = 4.5\,\mathrm{km\,s^{-1}}$ ($0.25 < \phi < 1.05$) rising briefly to $\delta v \sim 70\,\mathrm{km\,s^{-1}}$ ($\phi \sim 1.15$). The second is due to the spherical expansion and contraction of the photosphere, which when projected onto the line of sight and integrated over the stellar disk gives rise to the observed velocity variations. Since the line-of-sight amplitude varies from the center to the limb, line profiles integrated over the disk will be increasingly broadened and asymmetrical as the expansion (or contraction) velocity increases (Shapley & Nicholson 1919). Parsons (1972) found that pulsation-line broadening in classical Cepheids is small compared with instrumental and rotation broadening, but no equivalent line-profile calculations appropriate for helium star pulsations have been attempted. Finally, rotational broadening must also be considered.

The average line-width in the integrated spectrum was measured by isolating a small region containing strong narrow absorption lines around 4250 Å. The half-width half-maximum (HWHM) of the autocorrelation function (ACF) was measured. The procedure was repeated for a theoretical spectrum, broadened by increasing amounts to provide a calibration of the HWHM of the ACF. The broadening profile adopted was for rotation, but this was for convenience only. The true broadening is a convolution of instrumental (gaussian), integration time (top hats), rotation (elliptic) and asymmetric pulsation functions, but by measuring the width of the lines in terms of a single broadening parameter, the global broadening can be applied self-consistently when applying residual minimization techniques. The adopted value for "$v \sin i$" of $52 \pm 1\,\mathrm{km\,s^{-1}}$ is not a measure of the rotation velocity.

The coadded spectrum represents an average over the pulsation cycle of V652 Her. From ultraviolet analyses this pulsation is known to be approximately sinusoidal with an amplitude $\geq 2\,800\,K$ in effective temperature (Paper II) and this variation in $T_{\rm eff}$ will be folded into the absorption spectrum, to give an average effective temperature ($\overline{T_{\rm eff}}$). Due to unequal phase sampling (Fig. 1) the integrated spectrum for $\lambda > 4160$ Å, which dominates our analysis, is biased towards a mean phase $\phi = 0.95$, which is close to minimum radius and maximum temperature ($\phi \sim 0.1$). Hence $\overline{T_{\rm eff}}$ is likely to be greater than $\langle T_{\rm eff} \rangle$, the average value measured in Paper II. The phase-averaging may also have an effect on the measured surface gravity, $\overline{\log g}$, since the rapid acceleration phase lasting ~ 0.1 cycles around minimum radius, increases the effective gravity briefly by ~ 0.7 dex (Paper III). For this project the observed spectrum of V652 Her has been taken to represent some average photosphere for which self-consistent values of $\overline{T_{\rm eff}}, \overline{\log g}$, $v_{\rm t}$ and composition can be obtained.

3. Model atmospheres and synthetic spectra

The primary objective of this investigation was to establish the surface composition of V652 Her in a manner consistent with comparable studies of other extreme helium stars. Secondary objectives included a derivation of the average effective temper-

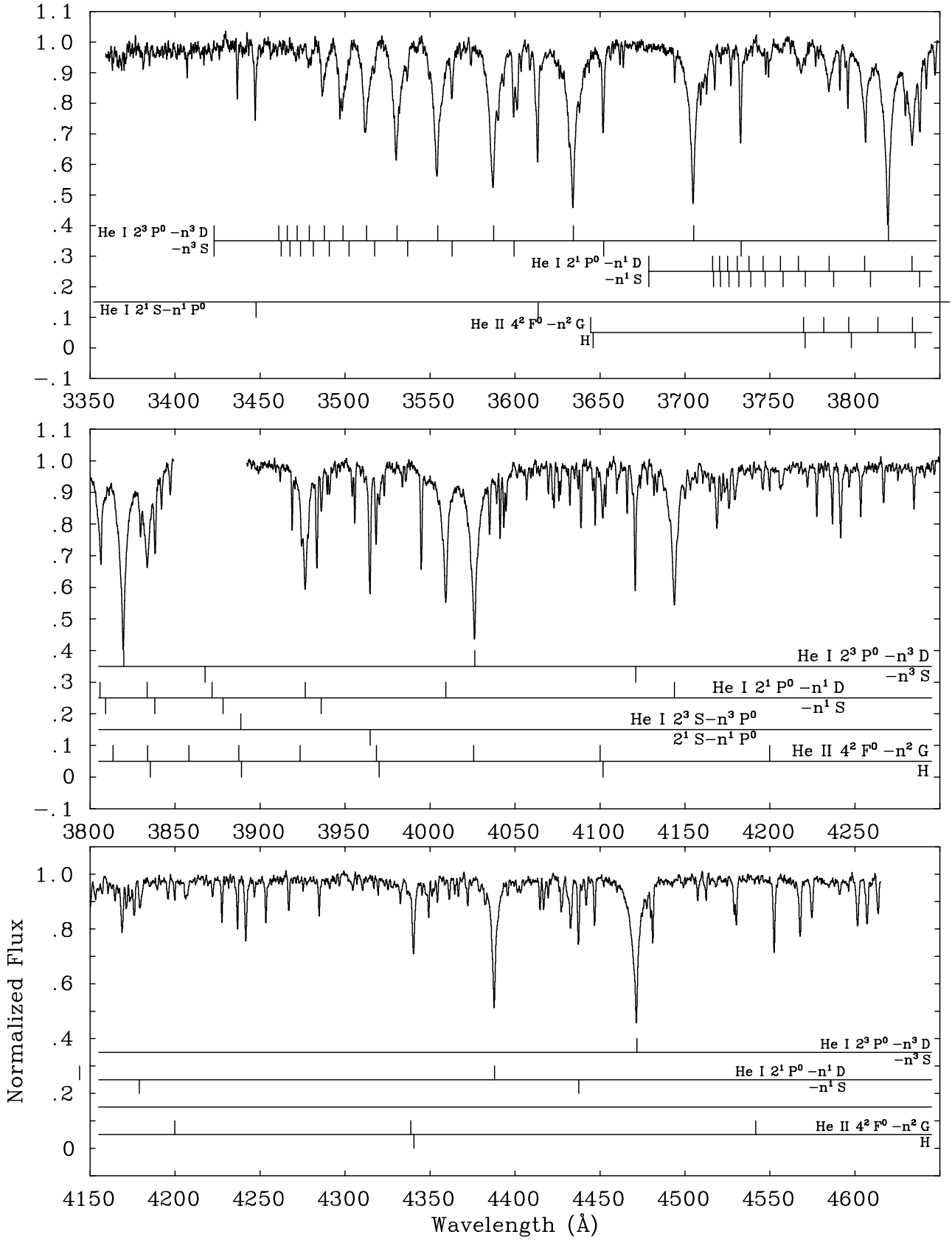

Fig. 2. The near-ultraviolet and blue spectrum of V652 Her, showing the positions of permitted helium and hydrogen lines and their series limits. The continuum placement for $\lambda < 4050$ Å is uncertain.

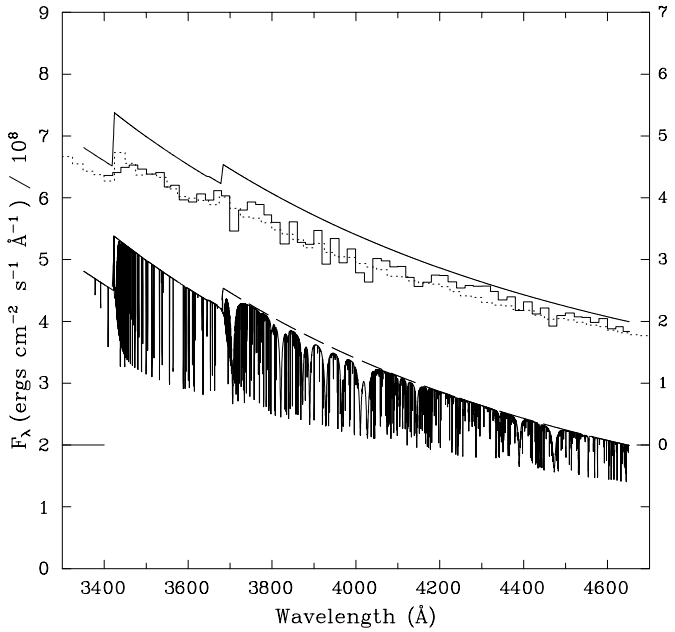

Fig. 3. The synthetic spectrum of a hydrogen-deficient stellar atmosphere with $T_{\rm eff} = 24\,000$ K, $\log g = 3.7$ calculated using SPECTRUM, together with the local continuum (lower plots). The upper plots show the same continuum flux, the same synthetic spectrum integrated into 20 Å bins (solid), and the emergent flux for the same model atmosphere predicted by the model atmosphere calculation STERNE (dotted). The upper plots are offset by 2.10^8 ergs cm^{-2} s^{-1} Å^{-1}. See the text for additional notes.

ature, the surface gravity and other quantities which may be deduced from the optical absorption spectrum. The latter are prerequisite to the former in the sense that any model atmosphere used to measure abundances should simultaneously reproduce all features of the absorption line spectrum. It is noted that the temperature and gravity thus derived are model-dependent quantities, representing those layers of the atmosphere in which the lines being studied and the local continuum are formed. Thus a model optimized to interpret the optical absorption spectrum may not necessarily provide a good reproduction of other features, such as the overall flux distribution or the ultraviolet absorption spectrum. Naturally, a perfect model containing a complete description of the physics of the model atmosphere will reproduce all observables at all times.

With this qualification in mind, line-blanketed model atmospheres have been calculated for V652 Her using STERNE, a computer code described in detail most recently by Jeffery et al. (1998). We have assumed that local radiative, thermodynamic and hydrostatic equilibria hold in the stellar atmosphere. The LTE approximation may be defended by analogy with early-type main-sequence B stars, where it has been shown (Anderson & Grigsby 1991) that the effects of line blanketing are more important than departures from LTE in determining the structure of the stellar atmosphere. The assumption of hydrostatic equilibrium was addressed in Paper III, where it was shown that the acceleration phase is long compared with the characteristic sound-wave transit of the atmosphere.

The composition adopted for the model atmospheres was based on a preliminary analysis by Jeffery et al. (1986) so that the relative abundances by number of hydrogen, helium and nitrogen were set to $n_{\rm H} = 0.01$, $n_{\rm He} = 0.98$ and $n_{\rm N} = 0.01$ respectively, with other species taking a solar abundance. A grid of models was constructed for $T_{\rm eff}$ between 20 000 and 30 000 K.

For comparison with observations, synthetic spectra were calculated using the LTE radiative transfer code SPECTRUM, most recently described by Jeffery et al. (1998). A significant improvement affecting the performance of this code restricted the wavelength region over which metal line opacities were calculated to within 50 Doppler widths of the line centre. A synthetic spectrum calculation including 566 transitions and 11 164 wavelength points between 3900 and 4600 Å now takes ~ 80 seconds on a Digital Alpha 500AU workstation. Several iterations of the procedures outlined below were necessary, the last involving the calculation of over 90 model atmospheres and 200 synthetic spectra.

The general properties of the synthetic spectra are illuminating. In Fig. 3 one model spectrum has been extended over the whole range of the observations. For illustrative purposes this model has not been degraded for instrumental or rotational broadening. Note that the metal line spectrum is much stronger than normally found in early-type stars of this temperature, a direct consequence of the low opacity in hydrogen-deficient atmospheres. It is also apparent that Stark broadening in the wings of neutral helium lines means that the continuum is not observed for $\lambda < 4050$ Å. High-order neutral helium lines have been included but without a full treatment of broadening, since appropriate data are not available. Thus at wavelengths $\lambda < 3750$ Å, the confluence of singlet and triplet series with the continuum is highly artificial (see Fig. 2). The synthetic spectrum also provides a useful check on the model atmosphere calculations, since the former should be equivalent to the flux emergent from the line-blanketed model atmosphere. This is seen to be approximately correct for the observed wavelength region in Fig. 3, although there is evidence that the existing hydrogen-deficient opacity distribution functions do not treat neutral helium adequately.

4. Photospheric parameters

The method of analysis adopted builds on that introduced into studies of helium star spectra by Jeffery et al. (1998), that of spectral synthesis. It has proceeded through many cycles beginning with the measurement of ionization equilibria from a few temperature senstive lines and the fitting of theoretical profiles to selected helium and hydrogen lines (Jeffery et al. 1986, Jeffery 1996). The ability to compute large sections of spectrum quickly has led to an increasing use of synthetic spectra to deduce fundamental properties of the stellar atmosphere. The major advantage of this method lies in showing how the entire spectrum responds to changes in a single quantity. The method greatly reduces errors introduced by blends and a tendency to rely on the strongest lines in the spectrum.

Having experimented with several methods, the effective temperature, surface gravity, and microturbulent velocity presented here were all measured by fitting grids of synthetic spectra to the observations. Thus, for example, the microturbulent velocity was obtained by adopting a theoretical model atmosphere with $T_{\rm eff}$ and $\log g$ close to that indicated in an earlier stage of the analysis. Synthetic spectra containing only O II lines were computed for a range of oxygen abundances ($n_{\rm O}$) and microturbulent velocities ($v_{\rm t}$). The root mean square residual between each model spectrum and the observed spectrum of V652 Her was formed, and its minimum value in the ($n_{\rm O}, v_{\rm t}$) plane was located. This provided the value $v_{\rm t} = 5 \pm 5\,{\rm km\,s^{-1}}$, which is similar to that obtained in LTE analyses of normal B stars.

Using a previous measurement of the chemical composition and this value for $v_{\rm t}$, a grid of synthetic spectra covering a large area in ($T_{\rm eff}, \log g$) space was calculated. These spectra include lines of all major species observed in the spectrum and for which the atomic data is reasonably reliable. Detailed linelists were described originally by Jeffery (1991), and are maintained on the WWW by Jeffery (1998, http://star.arm.ac.uk/∼csj/linelists.html). Each synthetic spectrum was corrected for broadening as described above.

The root mean square (rms) residual between these models and the observed spectrum was again measured, and the position of its minimum value in the ($T_{\rm eff}, \log g$) plane was located by interpolation. To improve the sensitivity of the rms residual to both temperature and gravity, two masks were applied to the residual before the rms value was calculated. The first mask represented the square of the difference between two synthetic spectra computed with different $T_{\rm eff}$, thereby emphasizing the contribution of temperature sensitive lines. The second mask cut out the cores of the He I λ4471, 4388 Å and all of He I λ4144 Å for reasons that are discussed in the next section and thereby improving the measurement of $\log g$.

Care was required to ensure that minimum value of the rms residual was correctly located. At minimum, the residual is nearly flat and smaller than the standard deviation in the mean over a range of 3000 K in $T_{\rm eff}$. It was therefore necessary to fit a parabola over a larger temperature range in order to locate the minimum reliably. The width of the parabola provides an error estimate since $T_{\rm eff}$ must lie within the 3000 K minimum ($\pm 3\sigma$) and hence $\sigma(T_{\rm eff}) = 500\,{\rm K}$. The minimum in $\log g$ is more tightly defined by the adopted grid ($\delta \log g = 0.2$) and no ambiguity results from adopting $\sigma(\log g) = 0.05$. These errors are approximately 2 to 3 times the formal errors and consistent with small variations arising from adjustments to various input parameters. For example, it became evident during the iteration of these solutions that small adjustments to the observed data were necessary and in particular to the radial velocity and continuum placement. The wavelengths of the observed spectrum were corrected by applying a radial velocity shift of 15 ${\rm km\,s^{-1}}$, measured by cross-correlation with a theoretical spectrum and simply removed a zero-point error introduced when constructing the original coadded spectrum. The rectified fluxes were multiplied by 1.01 to make a substantial improvement in fitting the theoretical continuum. Further wavelength-dependent adjustments to the rectification could arguably be justified, but only at the undesirable risk of allowing the models to guide the observations.

Using these values for $T_{\rm eff}$ and $\log g$, and using the same chemical composition as a reference, series of spectra were computed in which the abundance of each chemical species was varied over about 1 dex in increments of 0.15 dex. The minimum in the rms residual obtained for each series identified the best fit for the chemical composition. This procedure for the measurement $v_{\rm t}$, $T_{\rm eff}$, $\log g$ and chemical composition was iterated several times until complete consistency was achieved, yielding the basic photospheric parameters $T_{\rm eff} = 24\,550 \pm 500\,{\rm K}$, $\log g = 3.68 \pm 0.05$, $v_{\rm t} = 5 \pm 5\,{\rm km\,s^{-1}}$.

It has been noted that $v_{\rm t}$ has been measured primarily from O II lines. The effective temperature measurement results from the behaviour of ionization equilibria including He I/II, N II/III and Si II/III/IV, whilst the surface gravity measurement is dominated by the Stark-broadened wings of the diffuse He I lines 4471 and 4388 Å (Barnard et al. 1969, 1974, 1975). He I λ4026 Å is measured but not included in the fit procedure. Although the He I spectrum was observed to the $2^1{\rm P}^0$ and $2^3{\rm P}^0$ series limits[2], we do not have adequate atomic data to model the high-order lines correctly. It has so far been impossible to reproduce the cores of the He I lines. This problem is common to all contemporary studies of extreme helium stars. The helium line cores are formed at very low optical depths, $\log \tau_{4000} \sim -5$, where the current model atmospheres are sparsely sampled and numerically unreliable (see Jeffery et al. 1998).

The final solution for $T_{\rm eff}$, $\log g$ and $v_{\rm t}$ is shown in Table 2, and compared with the two similar helium stars discussed in Sect. 1. Although the internal errors are small, systematic errors from phase averaging and from the model atmospheres are

[2] One reason for observing the $2^1{\rm P}^0$ and $2^3{\rm P}^0$ series limits was to obtain an estimate of the electron density ($N_{\rm e}$) in the continuum-forming region of the atmosphere using the Inglis-Teller formula $\log N_{\rm e} = 23.26 - 7.5 \log n^*_{\rm m}$ (Inglis & Teller 1939), where $\log n^*_{\rm m}$ is the effective principal quantum number where the series merges with the continuum. $\log n^*_{\rm m}$ was estimated from each of the $2^1{\rm P}^0 - n^1{\rm D}$, $2^3{\rm P}^0 - n^3{\rm D}$ and $2^3{\rm P}^0 - n^3{\rm S}$ series by a regression on values of $\log r_0, \log n$, where r_0 is the residual intensity in the core of the helium lines. The values $\log N_{\rm e} = 14.52, 14.11, 14.49$ obtained from each series respectively are in all cases lower than the electron density in the model atmospheres with $\log g$ indicated by broadening theory, for which $\log N_{\rm e} = 14.84, 14.67$ at $\tau_{\rm cont} = 1$ for the singlet and triplet series respectively. Such a discrepancy has already been noted for the extreme helium stars HD 168476, HD 124448 and BD+10°2179 by Hill (1965). Given the very good fits obtained from broadening theory, it appears that the Inglis-Teller formula is of limited value in the study of helium star atmospheres. One likely reason is that the measurement of $n^*_{\rm m}$ depends on the residual intensities of severely blended broad lines which have been incorrectly normalized. Another may be that, since the formula is based on Holtsmark theory, it should probably be recalculated with theoretical He profiles which are not currently available. It is also appropriate to note that a more sophisticated theory of level dissolution described by occupation probabilities has been developed by Hummer & Mihalas (1988).

Table 2.

	V652 Her	V652 Her Lynas-Gray et al. 1984	LSS 3184 Drilling et al. 1998	HD 144941 Harrison & Jeffery 1997
$T_{\rm eff}$ (K)	$24\,550 \pm 500$	$23\,450 \pm 1320$	$23\,300 \pm 700$	$23\,200 \pm 500$
$\log g$ (cgs)	3.68 ± 0.05	3.70 ± 0.20	3.35 ± 0.10	3.9 ± 0.2
$v_{\rm t}$ (km s^{-1})	5 ± 5		15 ± 5	10

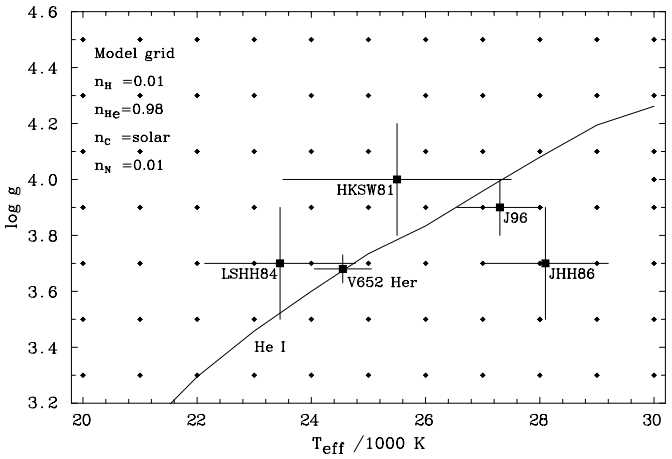

Fig. 4. A $\log g - \log T_{\rm eff}$ showing the position of the grid of model atmospheres (solid diamonds), the loci of optimum fits to He I lines, and the solutions for $T_{\rm eff}$ and $\log g$ for V652 Her in this and previous analyses. V652 Her = this paper, HKSW81 = Hill et al. 1981, LSHH84 = Lynas-Gray et al. 1984, J86 = Jeffery et al. 1986, J96 = Jeffery 1996.

likely to be more important for the absolute measurement of $T_{\rm eff}$, $\log g$. These should not affect the measurement of chemical composition significantly.

Previous measurements

Previous measurements of the average effective temperature and surface gravity have yielded $\langle T_{\rm eff}\rangle = 25\,500 \pm 2\,000$ K, $\log g = 4.0 \pm 0.2$ (Paper I), $\langle T_{\rm eff}\rangle = 23\,450 \pm 1\,320$ K, $\log g = 3.7 \pm 0.2$ (Paper II), $\overline{T_{\rm eff}} = 28\,100 \pm 1\,100$ K ($\log g = 3.7 \pm 0.2$ assumed, Jeffery et al. 1986) and $\overline{T_{\rm eff}} = 27\,300 \pm 750$ K, $\overline{\log g} = 3.9 \pm 0.1$ (Jeffery 1996) (Fig. 4). The first result was based on optical photometry, the second on ultraviolet spectrophotometry and model atmospheres which include line-blocking in the ultraviolet. The third and fourth results refer to the same spectrum analyzed here. The third is based on the ionization equilibrium measurement for Si II/IV, Si III/IV and N II/III but with continuum only model atmospheres. The fourth is based on the same equilibria but with line-blanketed model atmospheres. The new result improves on the latter two measurements by avoiding errors in the selection of line diagnostics and by treating the overlap of the helium-line profiles correctly.

The current measurements of $\overline{T_{\rm eff}} = 24\,550 \pm 500$ K, $\overline{\log g} = 3.68 \pm 0.05$ are close to the edge of the error ellipse for $\langle T_{\rm eff}\rangle$, $\log g$ given in Paper II. Since the average spectrum analyzed here is biased towards phases around minimum radius, it is sensible that $\overline{T_{\rm eff}}$ should be higher than $\langle T_{\rm eff}\rangle$. However, the anticipated value of $\overline{T_{\rm eff}}$ based on the Paper II results and on the phase distribution of Fig. 1 is $\sim 23\,600$ K, only marginally different from $\langle T_{\rm eff}\rangle = 24\,450$ K of Paper II. The discrepancy of nearly 1000 K is not entirely satisfactory but is within the experimental errors. Other factors, such as an incomplete treatment of line-blanketing in both Paper II and the present work, or an incorrect assumption of LTE and hydrostatic equilibrium approximations, could be responsible.

It should be noted that the spectra of V652 Her so far recorded omit the temperature-sensitive He II λ4686 Å line. Berger & Greenstein (1963) recorded the "doubtful" presence of this line in their 200-inch coudè spectrogram. New high-resolution observations including this line would thus help to define the effective temperature.

Table 3. Absorption lines between 4050 and 4615 Å in the model spectrum of V652 Her.

Ion	Lines	Lines/Blends >1 mÅ	Lines/Blends >10 mÅ	$\langle W_\lambda\rangle$ (Å)	$\sum W_\lambda$ (Å)
H I	2	2	2	0.3310	0.662
He I	11	11	11	0.8412	9.253
C II	29	5	0	0.0015	0.031
C III	18	3	0	0.0006	0.010
N II	98	58	50	0.0706	4.449
N III	11	9	4	0.0186	0.167
O II	147	87	60	0.0207	2.110
Ne II	23	18	4	0.0078	0.179
Mg II	6	5	4	0.0550	0.275
Al III	10	5	4	0.0737	0.442
Si II	7	3	2	0.0191	0.134
Si III	9	8	8	0.1009	0.807
Si IV	5	5	3	0.0428	0.214
P II	14	0	0	0.0002	0.002
P III	5	5	4	0.0358	0.179
S II	40	29	19	0.0139	0.501
S III	13	13	13	0.0579	0.753
Ar II	39	24	6	0.0065	0.208
Ca II	7	1	0	0.0008	0.005
Fe III	12	11	11	0.0497	0.547

5. Photospheric abundances

Table 3 shows the number of absorption lines due to each ion which contribute to the model spectrum within the wavelength

Table 4. Atmospheric abundances of V652 Her, two similar gravity helium stars and other extreme helium stars. Abundances are given (i) as $\log n$, normalised to $\log \Sigma \mu n = 12.15$ and (ii) as $[X/Fe] \equiv \log(\, n_{\rm X}/\, n_{\rm Fe})_\star - \log(\, n_{\rm X}/\, n_{\rm Fe})_\odot$, where the values adopted for [Fe] are shown in the final column.

Star	H	He	C	N	O	Ne	Mg	Al	Si	P	S	A	Fe	Ref.
(i)	$\log n$													
V652 Her	9.38	11.54	7.14:	8.93	7.54	8.38:	7.76	6.49	7.49	5.35	7.44	6.73	7.40	
σ	0.07		0.27:	0.06	0.08	0.40:	0.36	0.19	0.21	0.22	0.11	0.19	0.15	
LSS 3184	8.1	11.5	9.02	8.4	8.0			7.2	6.0	6.8	5.0	6.6	6.6	1
HD 144941	10.3	11.5	6.80	6.5	7.0			6.1	4.8	6.0			5.7	2
Sun	12.0	11.0	8.55	7.97	8.87	8.08	7.58	6.47	7.55	5.45	7.23	6.56	7.50	3
(ii)	[X/Fe]												[Fe]	
V652 Her	–2.52		–1.31:	1.06	–1.23	0.40:	0.28	0.12	0.04	0.00	0.31	0.27	–0.10	
LSS 3184	–3.20		1.16	1.05	–0.23		0.32	0.23	–0.05	0.20	0.10		–0.7	
HD 144941	0.13		0.09	0.30	–0.08		0.37	0.18	0.30				–1.9	
$\langle EHe \rangle$	-3.5		1.4	1.0	0.0		0.5	0.3	0.4	1.0	0.5			4

Notes. ":" = value uncertain, $\langle EHe \rangle$ represents a mean including the following stars: (1) HD16876, BD$+10^\circ 2179$, BD$-9^\circ 4395$, HD124448, LSE 78, LSS 3184.
References. 1: Drilling et al. 1998, 2: Harrison & Jeffery 1997, Jeffery & Harrison 1997, 3: Grevesse et al. 1996, 4: Jeffery 1996

region used for measuring abundances. The table also shows the number of lines or blends with equivalent widths (W_λ) exceeding 1 and 10 mÅ respectively, the average equivalent width per absorption line and the integrated equivalent width (in Ångström) for all absorption lines from each ion.

The final result of the fitting procedure is illustrated in Fig. 5. There is excellent correspondence in the wings of He I λ4471 Å and He I λ4388 Å and in the Hγ, δ profiles. Although He I λ4026 Å may not be correctly normalized, the model corresponds closely with the observed profile. Line broadening in He I λ4144 Å is inadequately treated. Other discrepancies may arise from noise in the observations, errors in definition of the local continuum, transitions missing from the synthetic spectrum and incorrect atomic data for individual lines.

The measured abundances of individual atomic species represented by absorption lines in the optical spectrum are given in Table 4. The errors in each measurement are difficult to assess using rms residual fitting as implemented. Here, we have taken the change in abundance required to produce an increase in the rms residual of 1% as an estimate of the 3σ error, leading to the 1σ values given in Table 4. These are comparable with the errors given in previous "line-by-line" studies such as Jeffery & Heber (1992). Systematic errors, for example, due to errors in $\log g$ and $T_{\rm eff}$, are comparable with those measured in detail for LSS 3184 (Drilling et al. 1998).

The carbon abundance has been measured from eight C II and C III lines with $1 < W_\lambda/{\rm m\AA} < 10$ and must be regarded as provisional. C II λ4267 Å is well known to yield consistently low abundances and has been excluded. Several Ne II lines are present between 4050 and 4615 Å. Although weak, they are stronger than the carbon lines and consistent with a normal cosmic abundance. Blending with unmodelled diffuse He I lines makes the stronger ultraviolet Ne II lines unusable. The stellar calcium H and K lines are obscured by a strong interstellar component, which has been smeared out by the velocity correction procedure. The abundances of magnesium, sulphur and argon appear to be anomalously high, and warrant further investigation.

6. Pulsation and evolution of V652 Her

Surface composition

The surface composition of V652 Her (Table 4) consists primarily of helium (98.8% by number), with nitrogen (0.25%) and hydrogen (0.9%). Carbon and oxygen are both well below the solar abundance.

It is clear that the helium has been produced as a result of nuclear hydrogen burning by the CNO process, since nearly all of the original carbon and oxygen has been converted to nitrogen. The amount of nitrogen observed is consistent with the original abundances of all three species being approximately solar. This is supported by the observed abundances for other species, including iron. There is also some residual hydrogen in the atmosphere, corresponding to a mixture (by mass) of 0.24% hydrogen-rich material and 99.76% CNO-processed material. The low carbon and oxygen abundances contrast strongly with the carbon-rich extreme helium stars in which 3α, $\mathrm{C}^{12}(\alpha,\gamma)\mathrm{O}^{16}$ and, possibly, other products are observed. The majority of species unaffected by CNO cycling, except magnesium, show abundances consistent with that expected from the iron and CNO abundances. This represents a substantial improvement over the analysis of Jeffery et al. (1986), who found an inexplicable overabundance of silicon (+1 dex). The result is also consistent with the pulsational instability observed in V652 Her. Saio's (1995) work indicated that, for pulsational instability, the metallicity Z must be greater than 0.01, whilst Fadeyev & Lynas-Gray (1996) find that a model with $Z = 0.01563$ satisfactorily reproduces the radial velocity

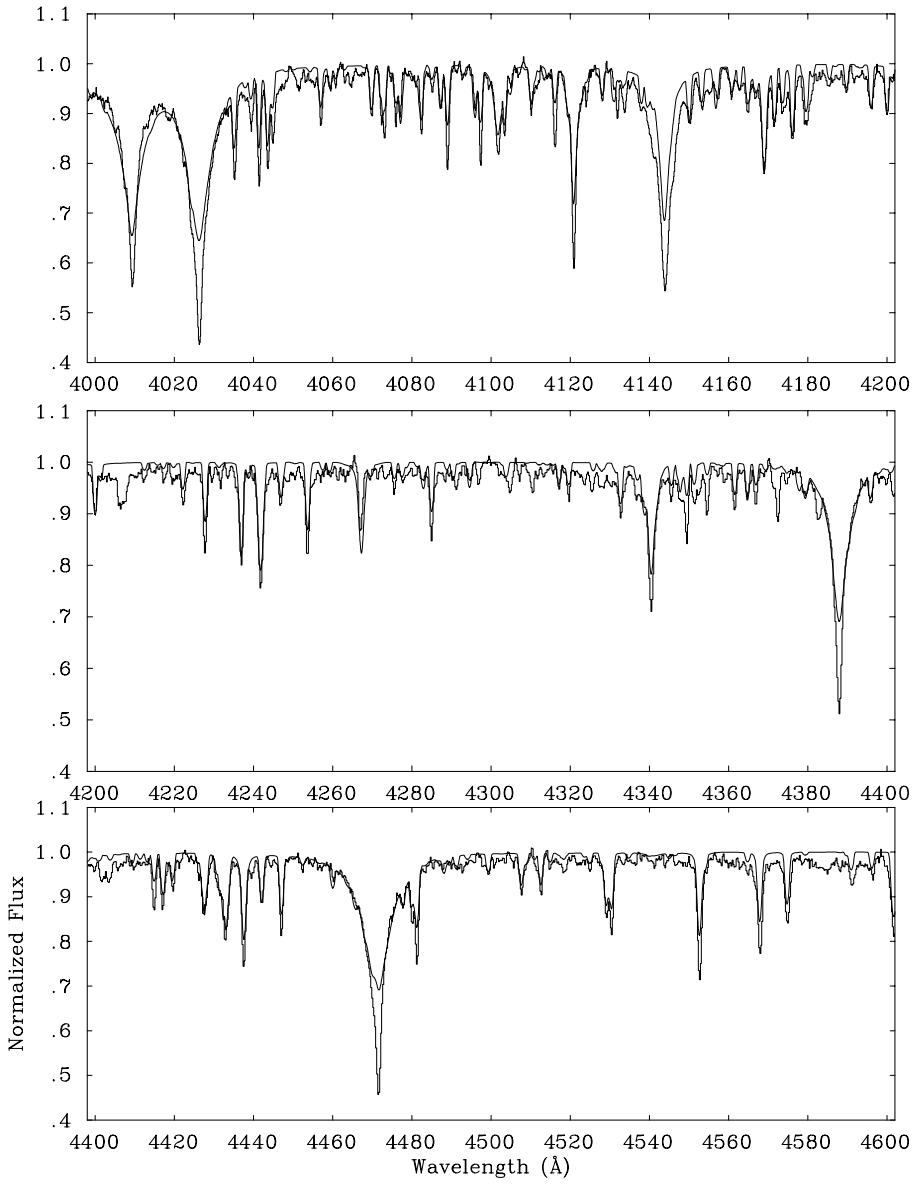

Fig. 5. Sections of the normalized spectrum of the pulsating helium star V652 Her are shown (histogram) together with the synthetic spectrum (smooth curve) calculated using the photospheric parameters and abundances given in Tables 2 and 4.

curve. The current abundance measurements translate to mass fractions $X = 0.0017, Y = 0.9825, Z = 0.0158$. These apparent consistencies should be treated circumspectly.

The two principle candidates for the progeny of carbon-rich extreme helium stars are (i) the merger of a carbon-oxygen and helium white dwarf binary following orbital decay by gravitational radiation (Webbink 1984, Iben & Tutukov 1985), and (ii) the reignition of a helium-burning shell during the late evolution of a post-asymptotic giant branch star towards the white dwarf cooling track (Iben et al. 1983). Since both candidates would produce a carbon-rich star, other possibilities must be explored for V652 Her. Jeffery (1984) constructed a series of artificial models for post-red giant branch stars with a fully mixed helium/hydrogen envelope surrounding a helium-burning core. By a judicious choice of parameters, several observed properties of V652 Her were reproduced. However, if the mass of V652 Her is as high as $0.7\,\mathrm{M}_\odot$ (Paper II), then it is difficult to explain how a red giant could accumulate $0.7\,\mathrm{M}_\odot$ of helium before core helium ignition. An alternative is to consider that V652 Her could be the result of a merger between two helium white dwarfs (Saio & Nomoto 1998). This model would have a predominantly CNO-processed surface and could account for the observed surface composition but, once again, is difficult to reconcile with the published mass.

Surface gravity and the mass of V652 Her

The measurements of relative and absolute radius variations enabled Lynas-Gray et al. (1984) to measure the average radius of V652 Her independent of distance ($\langle R \rangle = 1.98 \pm 0.21\,\mathrm{R}_\odot$). Together with the current value for $\overline{\log g} = 3.68 \pm 0.05$, this yields a mass of $M = 0.69^{+0.15}_{-0.12}\,\mathrm{M}_\odot$. This is satisfactorily close to the value $M = 0.7^{+0.4}_{-0.3}\,\mathrm{M}_\odot$ derived in Paper II. The improvement in the gravity measurement provided in the present paper

leads to a marked reduction in the error estimate, one of the original objectives of this project. It remains to be seen whether this value of $\overline{\log g}$ is sufficiently representative of the phase-averaged gravity that the derived mass is reliable. A critical phase-dependent study of $\log g$ and $T_{\rm eff}$, together with a fully consistent measurement of R, remains a priority for establishing the mass of V652 Her.

7. Conclusions

We have made a detailed analysis of the optical spectrum of the pulsating helium star V652 Her in order to measure an average effective temperature, surface gravity, and surface composition. With $T_{\rm eff} = 24\,550 \pm 500$ K, $\log g = 3.68 \pm 0.05$, $v_{\rm t} = 5 \pm 5$ km s^{-1}, the photospheric parameters are, to within observational errors, similar to results reported previously by Lynas-Gray et al. (1984). Together with a previous measurement of the mean stellar radius $\langle R \rangle = 1.98 \pm 0.21\,{\rm R}_\odot$, the new measurement of $\log g$ leads to an improved measurement of the mass of V652 Her, $M = 0.69^{+0.15}_{-0.12}\,{\rm M}_\odot$. The surface composition represents a mixture of 0.2% by mass of hydrogen-rich material, with 99.8% being CNO-processed helium. The abundances of species other than CNO represent those of a star with approximately solar metallicity, [Fe/H]$= -0.10 \pm 0.15$. All of these results are consistent with models of the pulsations of V652 Her, in which Z-bump opacities provide the driving mechanism.

Several problems need to be addressed. These include the carbon abundance, for which insufficient lines have been observed. Better normalization of the optical-ultraviolet spectrum, together with improvements in our treatment of diffuse He I lines towards the series limits, would enable us to refine the measurements of several species, including neon. Observations of He II λ4686 Å and Hβ will improve the measurements of $\langle T_{\rm eff} \rangle$ and hydrogen abundance. We have not attempted to redetermine the effective temperature from ultraviolet spectrophotometry, or to model the high-resolution ultraviolet spectrum obtained with IUE. New model atmospheres with opacity distribution functions more appropriate to the composition of V652 Her are required for this.

This analysis concludes a major effort to measure the chemical composition of V652 Her from observations obtained with what were high-sensitivity detectors close to the start of the modern telescope era. It has provided data which are essential to the detailed study of a unique pulsating helium star. Such studies can now be pursued with increased confidence, and can focus on more prosaic questions such as whether the LTE and hydrostatic approximations are valid in detail. To answer these, spectra with higher temporal and spectral resolution and higher signal-to-noise ratios will be required.

Acknowledgements. This research was supported initially through UK SERC grants to Dr P.W.Hill, subsequently through UK PPARC grants to Collaborative Computational Project No.7 for the Analysis of Astronomical Spectra, and latterly through financial support from the Department of Education in Northern Ireland to the Armagh Observatory.

References

Anderson L., Grigsby J.A., 1991, In: Crivellari L., Hubeny I., Hummer D.G. (eds.) Stellar Atmospheres: Beyond Classical Models. NATO ASI Series C, Kluwer, p. 365
Barnard A.J., Cooper J., Shamey L.J., 1969, A&A 1, 28
Barnard A.J., Cooper J., Smith E.W., 1974, JQSRT 14, 1025
Barnard A.J., Cooper J., Smith E.W., 1975, JQSRT 15, 429
Berger J., Greenstein J.L., 1963, PASP 75, 336
Drilling J.S., Jeffery C.S., Heber U., 1998, A&A 329, 1019
Fadeyev Yu.A., Lynas-Gray A.E., 1996, MNRAS 280, 427
Grevesse N., Noels A., Sauval A.J., 1996, In: Holt S.S., Sonneborn G. (eds.) Cosmic abundances. ASP Conf Ser. 99, 117
Harrison P.M., Jeffery C.S., 1997, A&A 323, 177
Hill P.W.., 1965, MNRAS 129, 137
Hill P.W., Kilkenny D., Schönberner D., Walker H.J., 1981, MNRAS 197, 81 (Paper I)
Hummer D.G., Mihalas D., 1988, ApJ 331, 794
Iben I. Jr., Tutukov A., 1985, ApJS, 58, 661
Iben I. Jr., Kaler J.B., Truran J.W., Renzini A., 1983, ApJ 264, 605
Inglis D.R., Teller E., 1939, ApJ 90, 439
Jeffery C.S., 1984, MNRAS 210 731
Jeffery C.S., 1991, Newsletter on Analysis of Astronomical Spectra No. 16, p. 17
Jeffery C.S., 1996, In: Jeffery C.S., Heber U. (eds.) Hydrogen Deficient Stars. ASP Conf Ser. 96, 152
Jeffery C.S., 1998, MNRAS 294, 391
Jeffery C.S., Harrison P.M., 1997, A&A 323, 393
Jeffery C.S., Heber U., 1992, A&A 260, 133
Jeffery C.S., Hill P.W., 1986, MNRAS 221, 975 (Paper III)
Jeffery C.S., Hill P.W., 1996, Observatory 116, 156
Jeffery C.S., Heber U., Hill P.W., 1986, In: Hunger K., Schönberner D., Rao N.K. (eds.) Hydrogen-deficient stars and related objects. IAU Coll. 87, Reidel, Dordrecht, Holland, p. 101
Jeffery C.S., Hamill P.J., Harrison P.M., Jeffers S.V., 1998, A&A 340, 476
Kilkenny D., 1988, MNRAS 232, 377
Kilkenny D., Koen C., 1995, MNRAS 275, 327
Kilkenny D., Lynas-Gray A.E., 1982, MNRAS 198, 873
Kilkenny D., Lynas-Gray A.E., 1984, MNRAS 208, 673
Kilkenny D., Marang F., 1991, IBVS No. 3660, 1
Kilkenny D., Lynas-Gray A.E., Roberts G., 1996, MNRAS 283, 1349
Landolt A.U., 1975, ApJ 196, 787
Lynas-Gray A.E., Schönberner D., Hill P.W., Heber U., 1984, MNRAS 209, 387 (Paper II)
Parsons S.B., 1972, ApJ 174, 57
Rogers F.J., Iglesias C.A., 1992, ApJS 79, 507
Saio H., 1986, MNRAS 221, 1P
Saio H., 1993, MNRAS 260, 465
Saio H., 1995, MNRAS 277, 1393
Saio H., Nomoto K., 1998, ApJ 500, 388
Shapley H., Nicholson S.B., 1919, Proc. Nat. Acad. Sci., 5, 417
Webbink R.F., 1984, ApJ 277, 355